COLLAGENOUS BONE MATRIX-INDUCED ENDOCHONDRAL OSSIFICATION AND HEMOPOIESIS

A. H. REDDI and WINSTON A. ANDERSON

From the Ben May Laboratory for Cancer Research and the Department of Anatomy, The University of Chicago, Chicago, Illinois. Dr. Reddi's present address is the Laboratory of Biochemistry, National Institute of Dental Research, National Institutes of Health, Bethesda, Maryland 20014. Dr. Anderson's present address is the Department of Zoology and Howard University Cancer Research Center, Howard University, Washington, D. C. 20059.

ABSTRACT

Transplantation of collagenous matrix from the rat diaphyseal bone to subcutaneous sites resulted in new bone formation by an endochondral sequence. Functional bone marrow develops within the newly formed ossicle. On day 1, the implanted matrix was a discrete conglomerate with fibrin clot and polymorphonuclear leukocytes. By day 3, the leukocytes disappeared, and this event was followed by migration and close apposition of fibroblast cell surface to the collagenous matrix. This initial matrix-membrane interaction culminated in differentiation of fibroblasts to chondroblasts and osteoblasts. The calcification of the hypertrophied chondrocytes and new bone formation were correlated with increased alkaline phosphatase activity and ^{45}Ca incorporation. The ingrowth of capillaries on day 9 resulted in chondrolysis and osteogenesis. Further remodelling of bony trabeculae by osteoclasts resulted in an ossicle of cancellous bone. This was followed by emergence of extravascular islands of hemocytoblasts and their differentiation into functional bone marrow with erythropoietic and granulopoietic elements and megakaryocytes in the ossicle. The onset and maintenance of erythropoiesis in the induced bone marrow were monitored by ^{59}Fe incorporation into protein-bound heme. These findings imply a role for extracellular collagenous matrix in cell differentiation.

There is growing knowledge about the intracellular molecules involved in cell differentiation (8). However, information pertaining to the possible role of extracellular matrix macromolecules such as collagen and proteoglycans has lagged (20). A characteristic feature of multicellular metazoa is the presence of extracellular matrix. In skeletal and dental tissues, extracellular matrices are most prominent and may provide important clues to their role.

On contact with demineralized collagenous matrices of bone and tooth, responding fibroblasts (mesenchymal cells) show an alteration of gene expression which results in emergence of new phenotypes (18, 19, 22, 32, 33). Simple techniques to study this phenomenon were developed and the temporal sequence of events were delineated (22). The importance of the physical dimensions of the matrix (18, 19, 23) and the surface charge characteristics (20, 24) in this process was demonstrated. Transplantation of powdered demineralized bone matrix, consisting predominantly of collagen in the

solid state, to subcutaneous sites resulted in new bone formation by an endochondral sequence. The new bone is occupied subsequently by functional bone marrow differentiating *in situ* (25). This paper presents correlated biochemical and electron microscope observations on this sequential biological cascade.

MATERIALS AND METHODS

Preparation and Transplantation of Matrix

Dehydrated diaphyseal shafts of rat femur and tibia were pulverized in a CRC Micro Mill (Chemical Rubber Company, Cleveland, Ohio) and sieved to a discrete particle size of 74-420 μm. The powders were demineralized with 0.5 M HCl and extracted with water, ethanol and ether, and prepared as described (22). Powders of this sort when plated on bacteriological agar plates did not reveal any bacterial colony.

Demineralized bone matrix was transplanted subcutaneously under ether anesthesia in male rats of Long-Evans strain, age 28-35 days (22). There were eight sites in the trunk at four symmetric locations: upper and lower thoracic, abdominal, and dorsal. About 25-30 mg of dry powder were implanted at each site with the aid of a blunt stainless steel spatula.

Alkaline Phosphatase and ^{45}Ca-Incorporation

On designated days of harvest, as indicated in Table I, $^{45}CaCl_2$ (sp act 11.2 mCi/mg) in saline was injected via a tail vein at a dose of 1 μCi/1 g body weight 4 h before termination of the experiment. At harvest, the transplantation plaque was weighed and portions were homogenized for alkaline phosphatase determination and ^{45}Ca incorporation, as described earlier (22), to quantitate the yield of new bone.

^{59}Fe Incorporation and Enzyme Assays

In order to precisely determine the onset of erythropoiesis during the *de novo* biogenesis of bone marrow in the newly formed ossicle, the incorporation of ^{59}Fe into protein-bound heme was determined as described earlier (25). Since earlier experiments revealed that the yield of bone marrow in the thoracic site is superior to that in the abdominal site, the present studies were restricted to the thoracic site (25). The results were expressed as cpm per milligram tissue. The femoral bone marrow served as an internal control. Under the conditions of the experiments, about 65–70% of the total protein-bound radioactivity was associated with the heme fraction.

At harvest, one-half of the plaque was weighed and homogenized in ice-cold 0.15 M NaCl containing 3 mM $NaHCO_3$ with the aid of a Polytron homogenizer (Brinkmann Instruments, Inc., Westbury, N.Y.) and centrifuged as described earlier (22). The supernates were used in the assay of acid phosphatase (EC 3.1.3.2) at a pH of 5.1 and alkaline phosphatase (EC 3.1.3.1) at a pH of 9.3, using *p*-nitrophenyl phosphate as substrate (10). 1 U of phosphatase activity was defined as the enzyme activity that liberated 1 μmol of *p*-nitrophenol in 0.5 h at 37°C per gram of tissue. Lactate dehydrogenase (EC 1.1.1.27) and malate dehydrogenase (EC 1.1.1.37) were determined spectrophotometrically (21). Total soluble protein was determined by the method of Lowry et al. (12), with bovine plasma albumin as a standard.

Electron Microscopy

The electron microscope studies were performed exclusively on transformation plaques from thoracic sites. Tissues were fixed in cold formaldehyde-glutaraldehyde fixative (11) for 60 min and then diced to 1-2 mm^3 and fixed for an additional 30 min. After rinsing in cold 0.1 M cacodylate buffer, pH 7.2, the samples were postfixed in cold 2% osmium tetroxide, dehydrated in graded ethanol solutions, and embedded in Epon. These sections with, and without, lead citrate staining were examined in a Siemens Elmiskop 101 electron microscope. Thick (1 μm) sections cut with an MT2 ultramicrotome were stained with Toluidine blue and employed for orientation purposes.

Endogenous Peroxidase Localization

Tissues were fixed for 60 min in formaldehyde-glutaraldehyde as described above, and the samples were washed overnight in 0.1 M cacodylate buffer pH 7.2. Sections (100-μm slices) were cut by an Oxford vibratome and incubated for 30 min at 37°C in 3.3'diaminobenzidine-H_2O_2 medium (pH 7.2) for localization of

FIGURE 1 Day 1. Collagen fibers showing typical cross-band periodicity in the implanted bone matrix. × 24,000. Inset (*a*) is a light micrograph showing the relationship of polymorphonuclear neutrophils (*n*) and fibrin (*f*) to the implanted matrix. × 200.

FIGURE 2 Day 1. A neutrophil in close proximity to the electron-dense fibrin and the implanted bone matrix is revealed in this micrograph. × 16,000. The inset (*a*) shows the characteristic banded structure of fibrin. × 35,000.

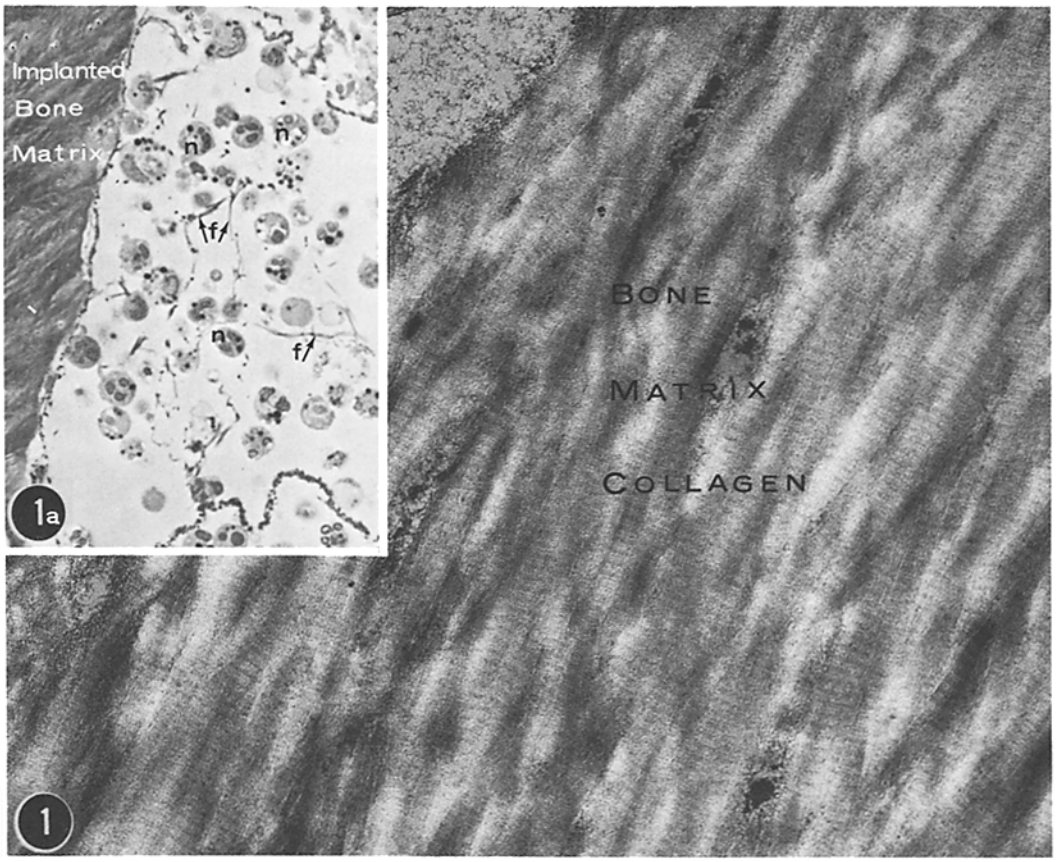
Implanted
Bone
Matrix
n
n
f
n
f
1a
BONE
MATRIX
COLLAGEN
1

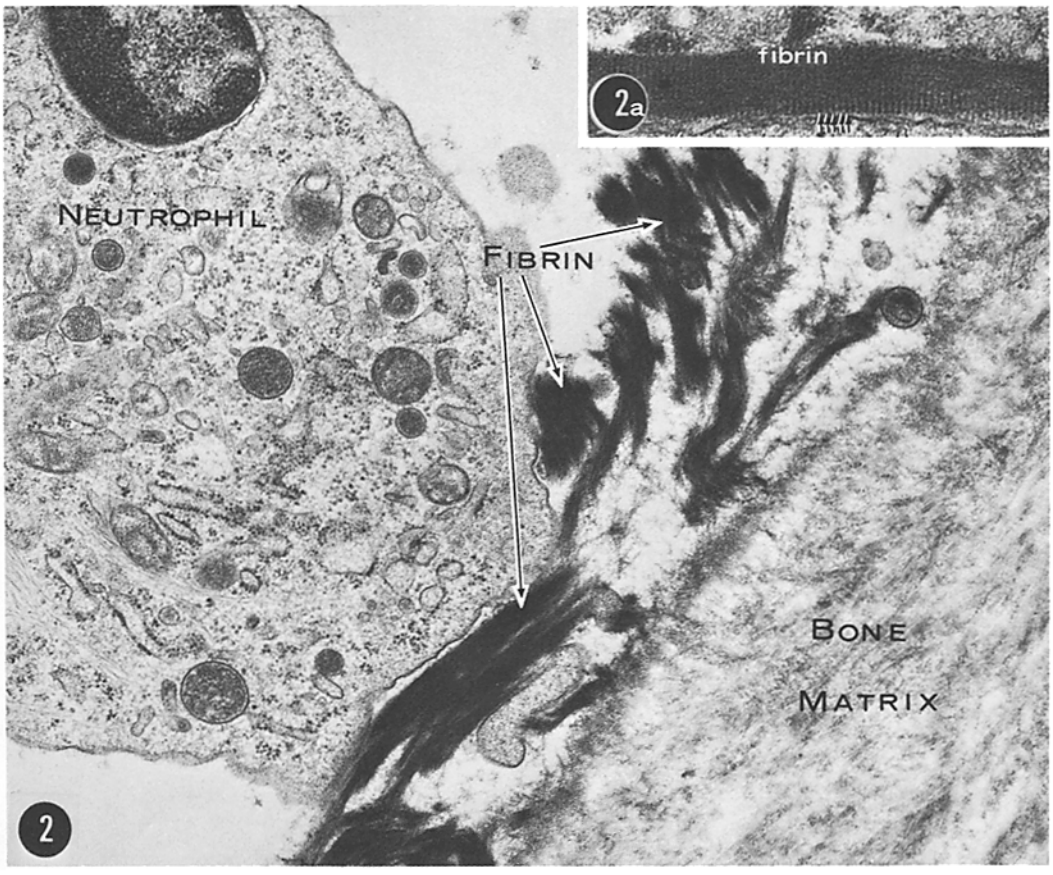
fibrin
2a
NEUTROPHIL
FIBRIN
BONE
MATRIX
2

endogenous peroxidase (7). After a brief rinse, the slices were osmicated, dehydrated, and embedded in Epon. These sections were stained lightly with lead citrate (26) and examined.

RESULTS

Sequential Changes

Transplantation of powdered demineralized diaphyseal bone matrix to thoracic sites in allogeneic recipients resulted in the formation of a discrete transformation plaque within 24 h. The implanted matrix revealed the typical cross striations of collagen (Fig. 1). On day 1, the plaque was a compact conglomerate of the implanted matrix and irregular strands of fibrin and polymorphonuclear leukocytes (Fig. 1 *a*). Alkaline phosphatase, a characteristic enzyme of rat polymorphonuclear leukocytes (15), was detected in the plaque (Table I). The fibrin was electron dense and of various lengths and exhibited a banded pattern with about 250 Å periodicity (3, 17). The polymorphonuclear neutrophilic leukocytes phagocytized the fibrin and cell debris (Fig. 2). Some cells appeared to migrate toward the implanted matrix (Fig. 3). Many leukocytes contained lysosomes with membranous inclusions (Fig. 4). By day 3, most leukocytes disappeared. This event was correlated with decline in alkaline phosphatase activity in the plaques (Table I).

On days 3 and 4, numerous elongate fibroblast-like cells appeared in close proximity to the implanted matrix (Figs. 5, 6 and 6 *a*), and some of the cell processes appeared to invade the crevices in the matrix (Fig. 7). There was a close initial interaction between the fibroblast plasma membrane and the surface of the matrix (Fig. 7). There was no evidence of phagocytosis of matrix material by fibroblasts.

On day 5, the first chondroblasts appeared. These cells were numerous by days 7 and 8 (Fig. 8

TABLE I

Changes in Alkaline Phosphatase Activity and ^{45}Ca Incorporation in Transformation Plaques

Day	Alkaline phosphatase	^{45}Ca incorporation	Histology
	U/g	*cpm/mg*	
1	5.2 ± 0.7	ND	Polymorphonuclear leukocytes ++
3	3.1 ± 0.4	26 ± 6	Polymorphonuclear leukocytes +
			Fibroblasts ++++
5	3.2 ± 0.4	51 ± 8	Fibroblasts +++
			Chondroblasts +
7	25.0 ± 2.8	351 ± 190	Chondrocytes +++
9	19.6 ± 3.1	1,790 ± 460	Hypertrophy and calcification of chondrocytes
			Capillary ingrowth
10	45.7 ± 9.3	2,956 ± 764	Chondrolysis
			Osteoblasts +++
11	47.0 ± 8.7	6,144 ± 1,956	Bone +++
14	27.8 ± 3.4	5,012 ± 458	Bone +++
			Early hemocytoblasts
18	32.5 ± 4.2	4,330 ± 703	Bone ++++
			Bone marrow ++
21	30.8 ± 2.8	6,778 ± 739	Bone ++++
			Bone marrow ++++

ND, not detectable; ±, Standard error of mean of eight observations.

FIGURE 3 Day 2. A penetrating cell with close approximation of the cell membrane to the implanted matrix is revealed. × 12,000.

FIGURE 4 Day 3. A neutrophil located close to implanted matrix contains numerous lysosomes (L_1-L_6) with degenerating membranous inclusions. × 8,000.

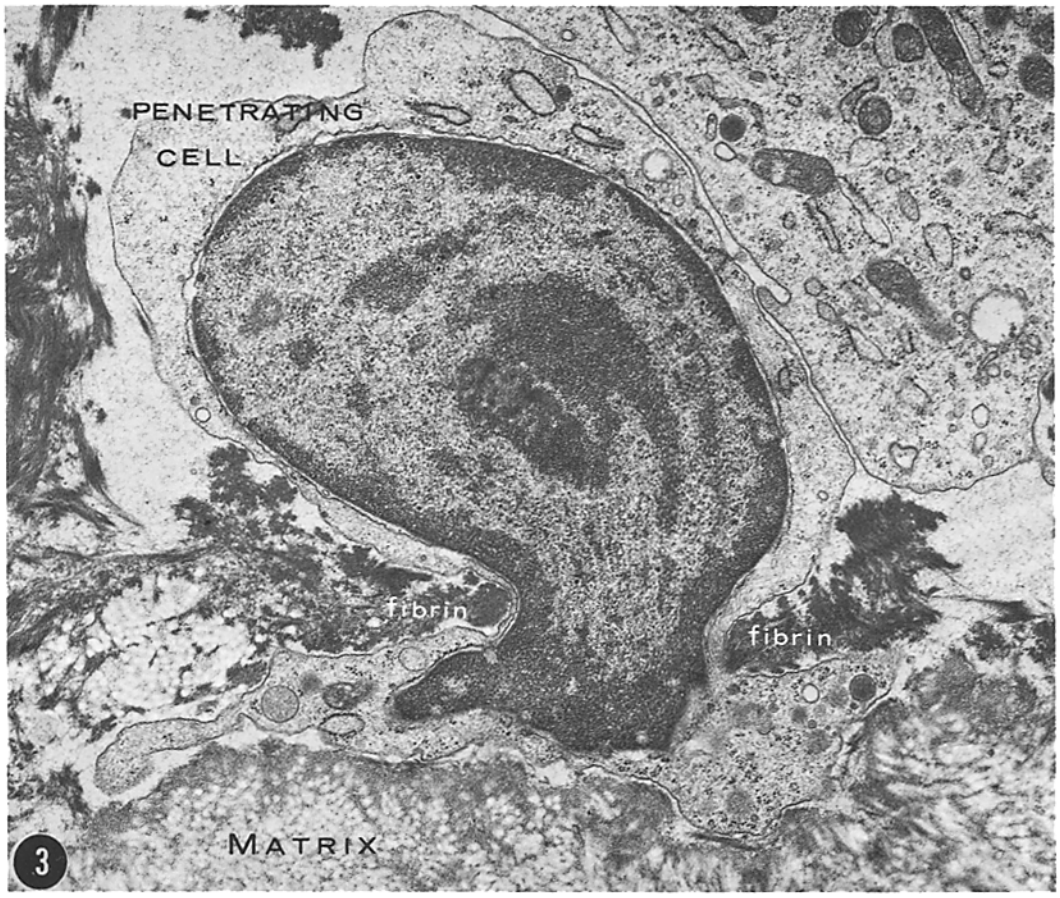
PENETRATING
CELL
fibrin
fibrin
MATRIX
3

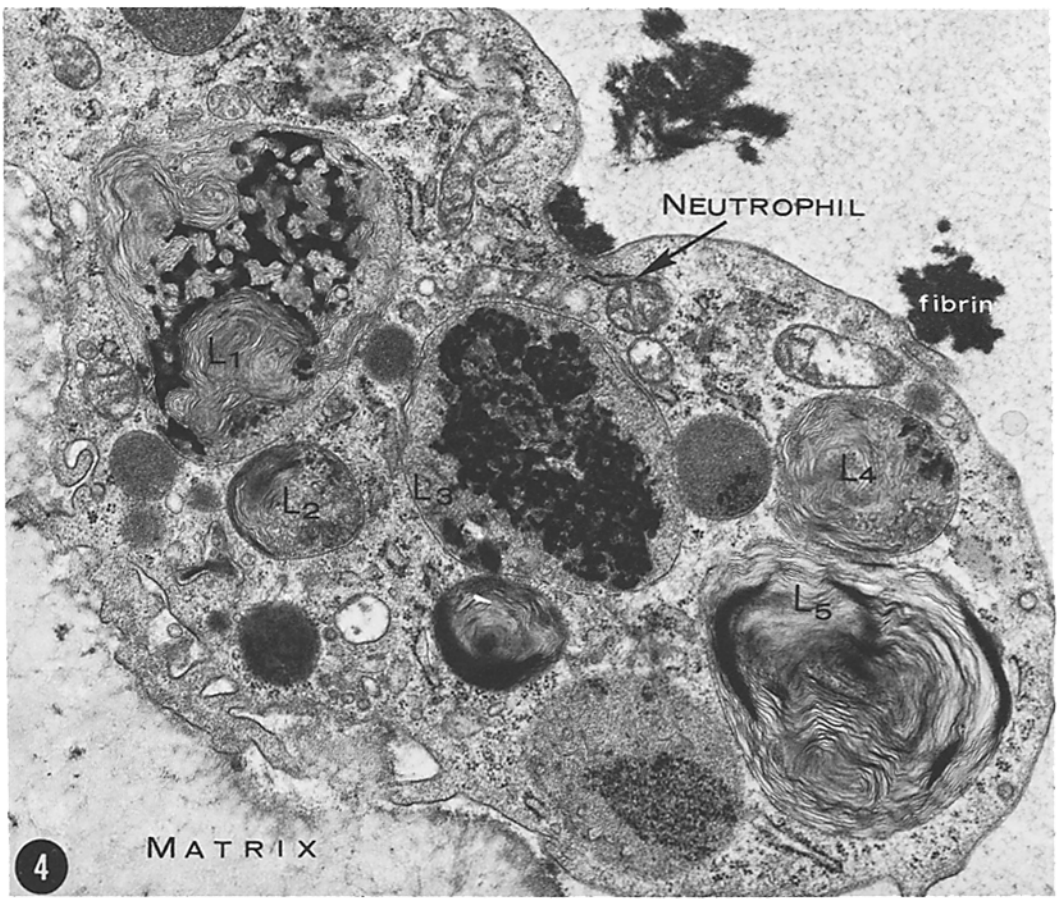
NEUTROPHIL
fibrin
L1
L2
L3
L4
L5
MATRIX
4

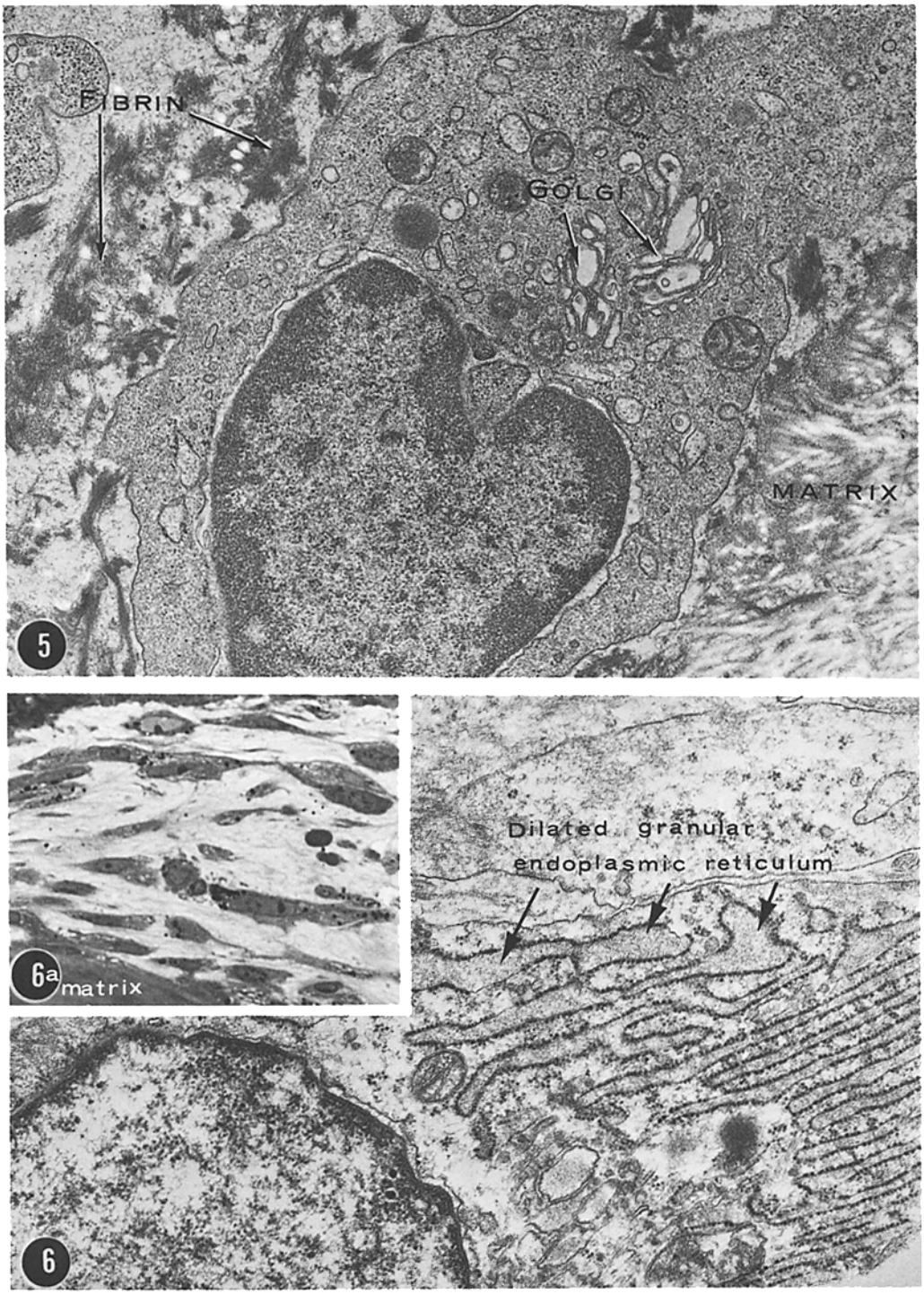

FIGURE 5 Day 3. A cell with well-developed Golgi apparatus is located in close proximity to the implanted matrix. Fragments of fibrin persist. × 12,000.

FIGURE 6 Day 4. Elongate fibroblastic cells (*a*) containing well-developed granular endoplasmic reticulum are located in the region of the implanted bone matrix. × 14,000.

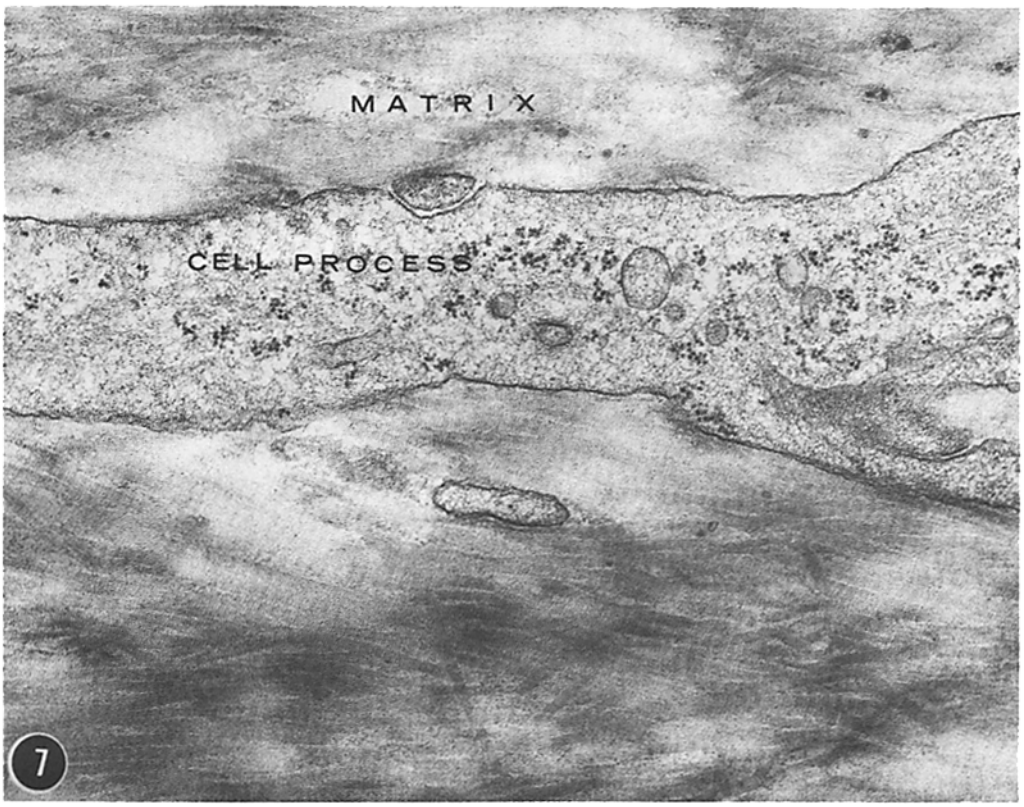

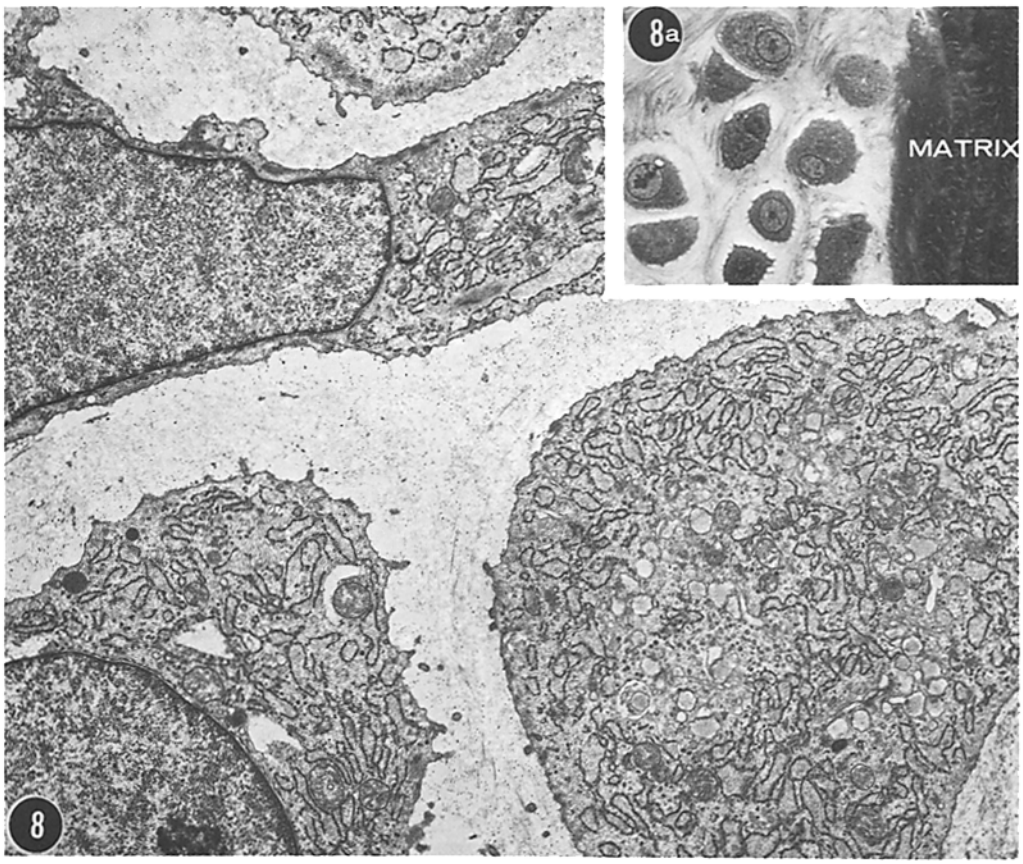

FIGURE 7 Day 5. A cell process from the fusiform fibroblastic cell appears in close apposition to the implanted collagenous bone matrix. × 20,000.

FIGURE 8 Day 7. Chondroblasts with well-developed granular endoplasmic reticulum adjacent to the implanted matrix. Cartilage matrix with filamentous meshwork is also observed. × 3,000.

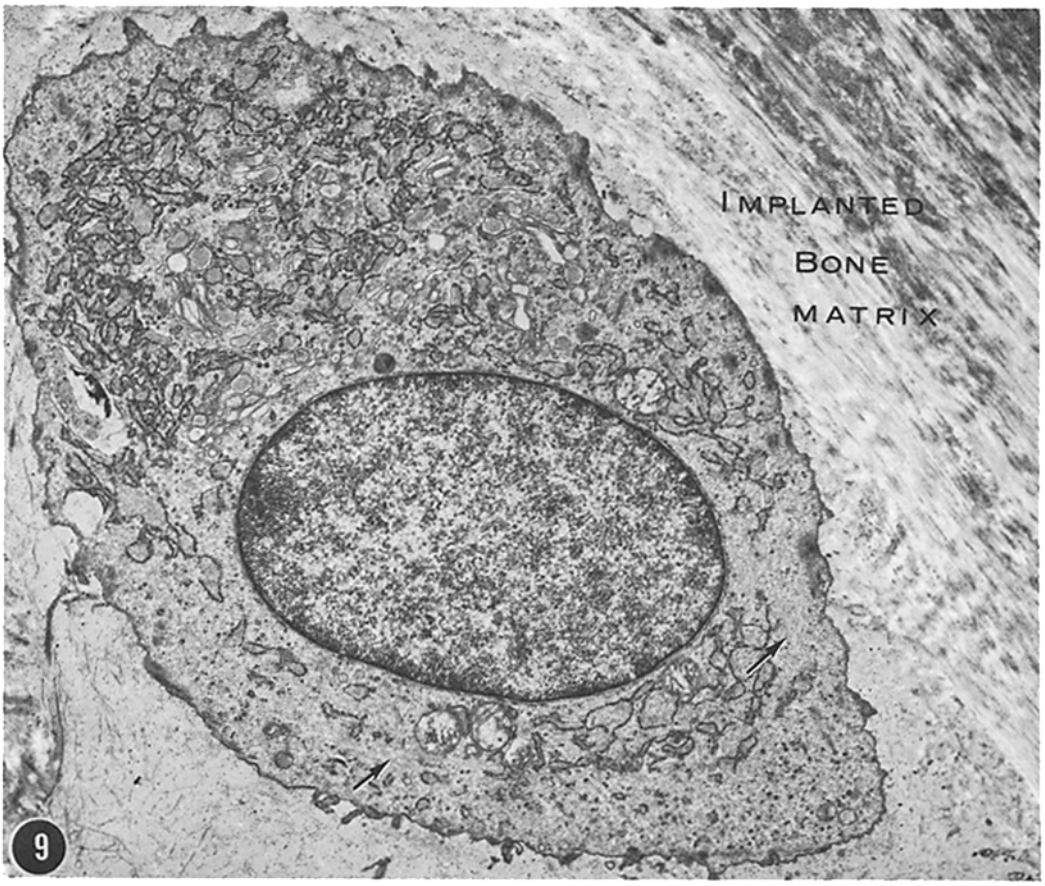

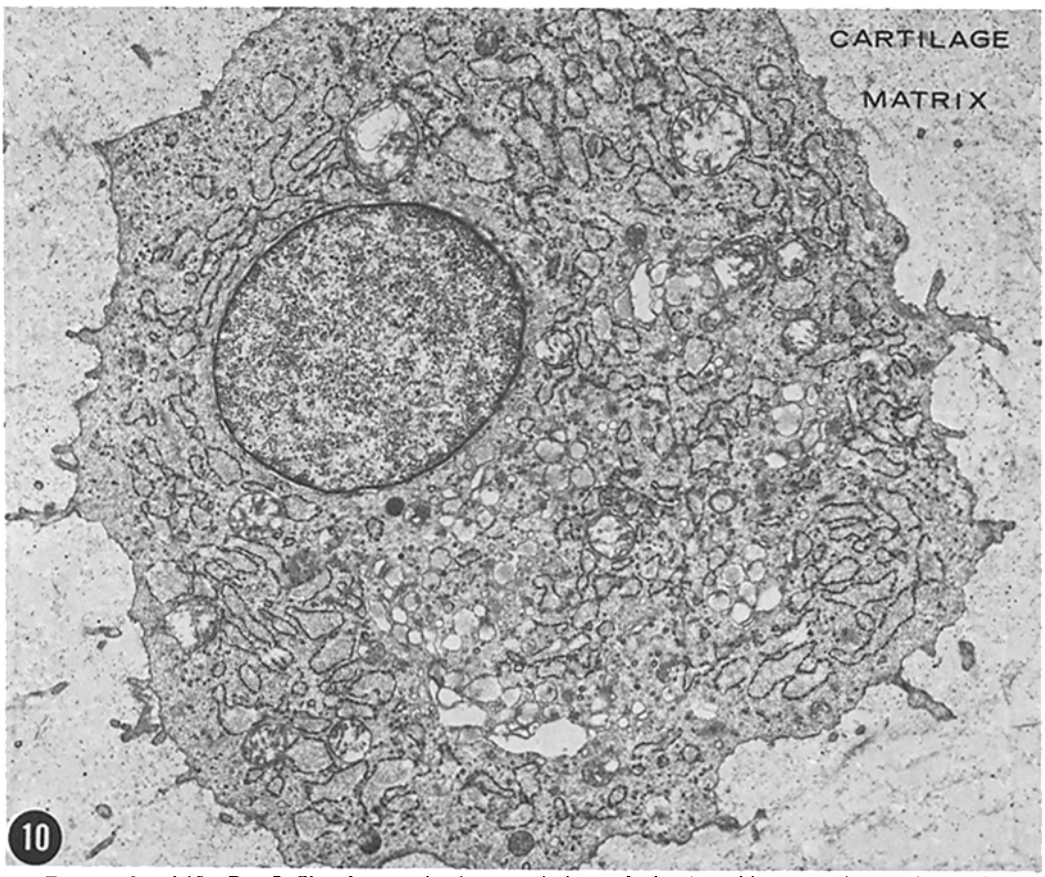

FIGURES 9 and 10 Day 7. Chondrocytes in close proximity to the implanted bone matrix reveal extensive dilated granular endoplasmic reticulum. Well-developed cartilage matrix surround these cells. Arrows in Fig. 9 indicate the characteristic cytoplasmic fibrils. × 8,000.

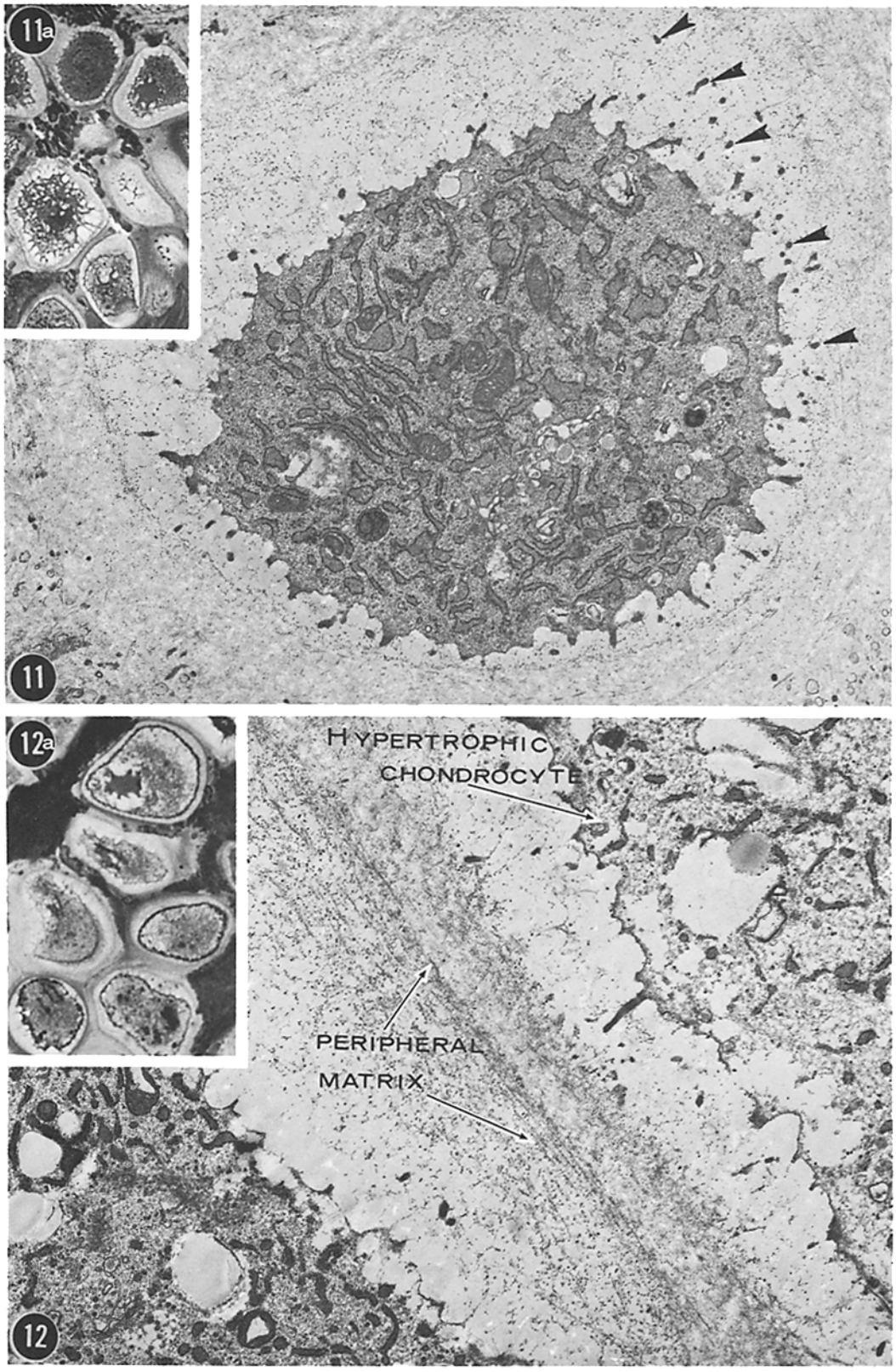

FIGURE 11 Day 9. Hypertrophic chondrocytes in well formed lacunae are revealed in this micrograph (*a*). × 600. In a corresponding electron micrograph, the hypertrophic chondrocytes are shown with numerous electron-dense cell processes that extend into the cartilage matrix (arrows). × 6,400.

FIGURE 12 Day 9. This electron micrograph illustrates the late stages of the hypertrophic chondrocytes with extensive degradation of cytoplasmic organelles and fragmentation of cell membrane. A fibrous network in the peripheral matrix is revealed. × 8,000. Inset (*a*) is a corresponding light micrograph exhibiting pyknotic nuclei in hypertrophic chondrocytes. × 600.

and 8 *a*). The chondrocytes exhibited a round or oval nucleus and a well-developed granular endoplasmic reticulum and Golgi region (Figs. 9 and 10). Another characteristic feature of the chondrocytes was the occurrence of numerous cytoplasmic fibrils (Fig. 9). The chondrocytes were closely juxtaposed to the implanted matrix (Fig. 9). These cells were separated by well-developed matrix composed of both granular and fibrillar material. Correlated experiments revealed considerable incorporation of ^{35}S into chondroitin sulfate (22).

The chondrocytes hypertrophied and there was extensive fragmentation of the cell processes (Figs. 11, 12, and 12 *a*). Also present in the extracellular matrix were numerous dense bodies similar to matrix vesicles (1, 2). With further hypertrophy on day 9, the nuclei were pyknotic and there was degeneration of the cytoplasm (Fig. 12). Immediately adjacent to the hypertrophic chondrocyte was a "halo" surrounded by a fibrous network with dense granules (Figs. 11 and 12). The first signs of mineral formation were evident both near the surface of the hypertrophied chondrocyte and in the peripheral matrix (Fig. 13). With the advent of sprouting capillaries on day 9, several chondrolytic foci were evident. By day 10, numerous multinucleate chondroclasts appeared close to regions of chondrolysis. Osteoblasts with intense basophilia appeared close to the vascular endothelium and exhibited well-developed granular endoplasmic reticulum (Fig. 14 and 14 *a*). New bone formed by appositional growth on the surface of the calcified cartilage matrix and the implanted nonliving collagenous matrix. The initial events of calcification of cartilage and emergence of osteoblasts correlated with increased deposition of bone mineral and marked increases in alkaline phosphatase activity followed by ^{45}Ca incorporation (Table I).

The disappearance of cartilage on days 10 and 11 resulted in a corresponding decline in lactic dehydrogenase (LDH) activity (Table II). From day 11 onwards, there was increased mineralization and ^{45}Ca incorporation (Table I). Extensive remodelling of the new bone was associated with the presence of osteoclasts (6) with characteristic ruffled border in close proximity to the mineral phase (Fig. 15 and 15 *a*).

By day 12, the chondrolysis was almost complete and the plaque consisted of an irregular honeycomb of trabeculae of bone and cavernous sinuses lined with flattened cells. The first loci of hemopoiesis were in the form of extravascular islands of small basophilic cells and primitive granulocytes. On days 14 to 16 there was vascular confluence, and the sinuses were crammed with erythrocytes, presumably preformed, as indicated by low values for ^{59}Fe incorporation (Table II).

Between days 16 and 21 there was further remodelling of the bone, and the roughly ovoid ossicle was filled almost entirely with bone marrow elements including erythrocytic and granulocytic series and megakaryocytes. As seen in Table II, about 6–7 days after the first signs of hemopoietic precursor cells, erthropoiesis as indicated by ^{59}Fe incorporation into heme was significantly increased and attained a plateau by day 24 and remained at this level up to day 70. The developing erythrocytes displayed diaminobenzidine staining for hemoglobin. The neutrophils exhibited a reaction product for endogenous peroxidase in discrete cytoplasmic granules and in dilated cisternae of the endoplasmic reticulum (Figs. 16–18). The full development of hemopoietic bone marrow correlated with the increased activities of lactic and malic dehydrogenases. The increasing acid phosphatase activity may be due to erythropoiesis (13), and the alkaline phosphatase activity may reflect myelopoiesis (Table II).

DISCUSSION

The formation of cartilage, bone, and bone marrow in response to subcutaneous implantation of powders of nonliving collagenous diaphyseal bone matrix is reminiscent of the embryonic differentia-

FIGURE 13 Day 10. Illustrates the formation of electron-dense deposits of mineral close to cell membrane of the hypertrophied chondrocyte and in the peripheral matrix. × 8,000.

FIGURE 14 Day 11. Osteoblasts (*ob*) with characteristic basophilia following Toluidine blue staining are shown next to the bone matrix (*a*). Electron micrograph reveals extensive granular endoplasmic reticulum (Fig. 14). Note the new collagen immediately surrounding the cell and extensive mineralization of new bone matrix. × 20,000.

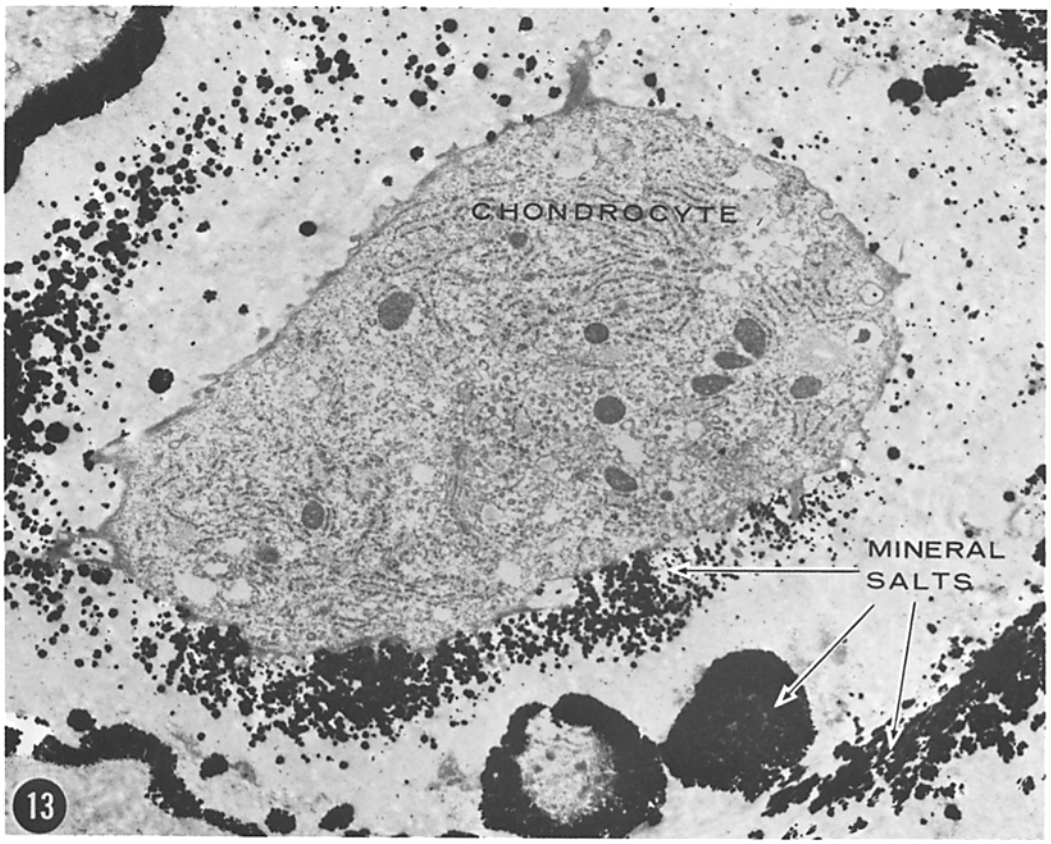
CHONDROCYTE
MINERAL
SALTS
13


ob
14a
bone

OSTEOBLAST
BONE
14

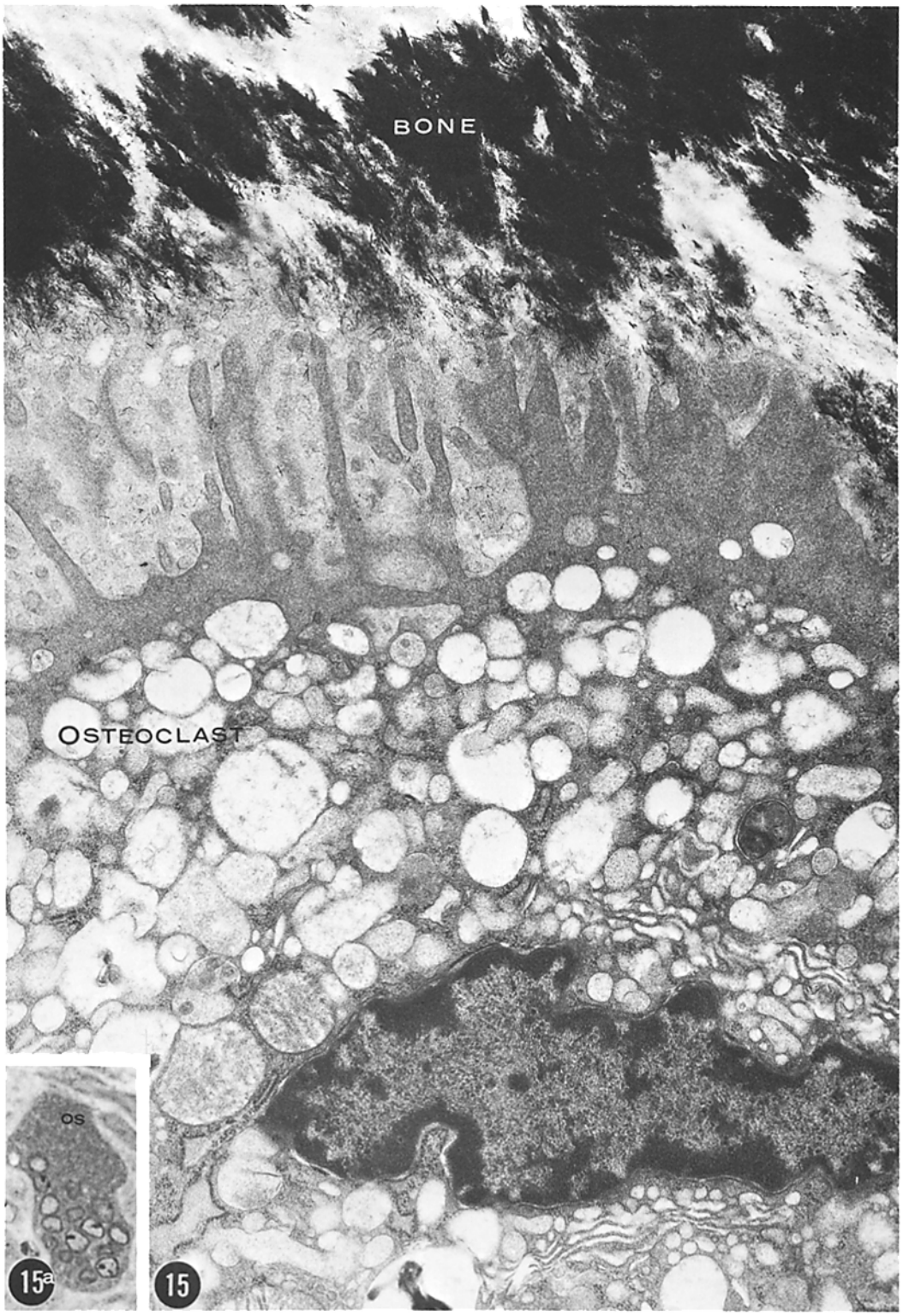

FIGURE 15 Day 18. Multinucleated osteoclast (*oc*) is depicted in inset (*a*). Corresponding electron micrograph reveals the ruffled cell border close to the bone mineral and matrix. × 16,500.

TABLE II

Phosphatases, Dehydrogenases, and ^{59}Fe-incorporation in Transformation Ossicles

Day	Phosphatases		Dehydrogenases		Soluble protein	^{59}Fe-incorporation
	pH 5.1	pH 9.3	Lactate	Malate		
	U/g	*U/g*	*U/g*	*U/g*	*mg/g*	*cpm/mg*
9	16.3 ± 0.6	47.4 ± 3.8	21.6 ± 2.4	19.3 ± 2.0	18.4 ± 0.5	ND
12	19.9 ± 2.0	38.4 ± 5.3	11.7 ± 1.3	10.0 ± 1.1	19.5 ± 1.0	ND
14	22.0 ± 3.5	52.5 ± 3.3	15.9 ± 1.1	13.2 ± 0.7	17.5 ± 0.6	1 ± 0.2
16	24.9 ± 2.8	47.7 ± 3.4	15.1 ± 1.9	18.1 ± 3.3	20.8 ± 1.2	4 ± 2
18	43.9 ± 4.5	49.3 ± 2.4	14.5 ± 1.0	17.9 ± 1.3	24.7 ± 1.5	10 ± 4
20	85.0 ± 5.8	39.1 ± 1.3	30.6 ± 5.5	28.1 ± 3.1	32.3 ± 1.7	130 ± 19
21	36.3 ± 5.0	40.8 ± 3.0	16.6 ± 2.1	18.9 ± 2.0	27.3 ± 1.6	218 ± 47
24	29.7 ± 2.9	35.2 ± 2.3	20.8 ± 2.7	26.7 ± 2.7	24.6 ± 1.9	343 ± 81

ND, not detectable; ±, Standard error of mean; n = 8 for all determinations.

tion of these tissues. The early events include formation of blood clot and emigration of polymorphonuclear leukocytes. The chemotaxis for leukocytes in response to collagenous matrix is not due to bacterial contamination since sterilized matrix yielded identical results. This inflammation-like response is a transient event and is followed by migration and adhesion of fibroblasts in contiguity with the implanted matrix. These initial matrix-membrane interactions result in alteration of gene expression in responding fibroblasts and culminates in the appearance of new phenotypes. The precise mechanisms underlying this transformation of phenotype is not known. However, the surface charge (19, 24) and geometry of the matrix (19, 23) are critical. Moreover, there is a stringent specificity among the collagenous matrices tested (18–20). Only bone and tooth matrices are active; inactive collagenous matrices include tendon, skin, and cartilage.

Studies by Slavkin (30) on differentiation of tooth implicated RNA in induction. However, in the present study treatment of the matrix with RNAase or DNAase before subcutaneous implantation did not influence the biological response (20). Pretreatment of the matrix with bacterial collagenase, trypsin, and papain abolished the observed phenotype changes (20). It would appear that the integrity of the helical and nonhelical domains of collagenous matrix is essential. The likelihood of a molecule covalently linked to collagenous matrix as the putative mediator is suggested by experiments with sulfhydryl reducing agents dithiothreitol and mercaptoethanol (20). The alternate possibility that the reducing agents perturb the conformation of a critical region in the matrix should not be overlooked. The short-range contact-mediated nature of the cellular response is best explained by a matrix-associated insoluble molecule. It is, therefore, likely that collagenous matrix may aid in restricting the mobility of morphogenetically crucial molecules. Other matrix molecules such as phosphoproteins, hyaluronate, and sialoproteins were ruled out by experiments involving pretreatment of the matrix with acid and alkaline phosphatases, hyaluronidase, and neuraminidase (20).

The sequential changes during matrix-induced chondrogenesis, chondrolysis, and osteogenesis are analogous to those described in differentiating tissues (4, 5, 14, 28, 29, 31). The early events in biogenesis of bone marrow and the morphology of hemopoietic elements are similar to those of medullary bone marrow (3, 16).

There is an excellent correlation between increasing alkaline phosphatase activity (27) and calcification as indicated by ^{45}Ca incorporation into the mineral phase and the electron microscope localization of electron-dense mineral. The incorporation of ^{59}Fe into protein-bound heme paralleled the appearance and proliferation of erythropoietic elements.

The cascade of events and the temporal sequence during the matrix-induced bone formation are similar to those observed during fracture healing in long bones (9). In view of this, it is conceivable that the collagenous matrix may play an important role in specifying morphogenetic

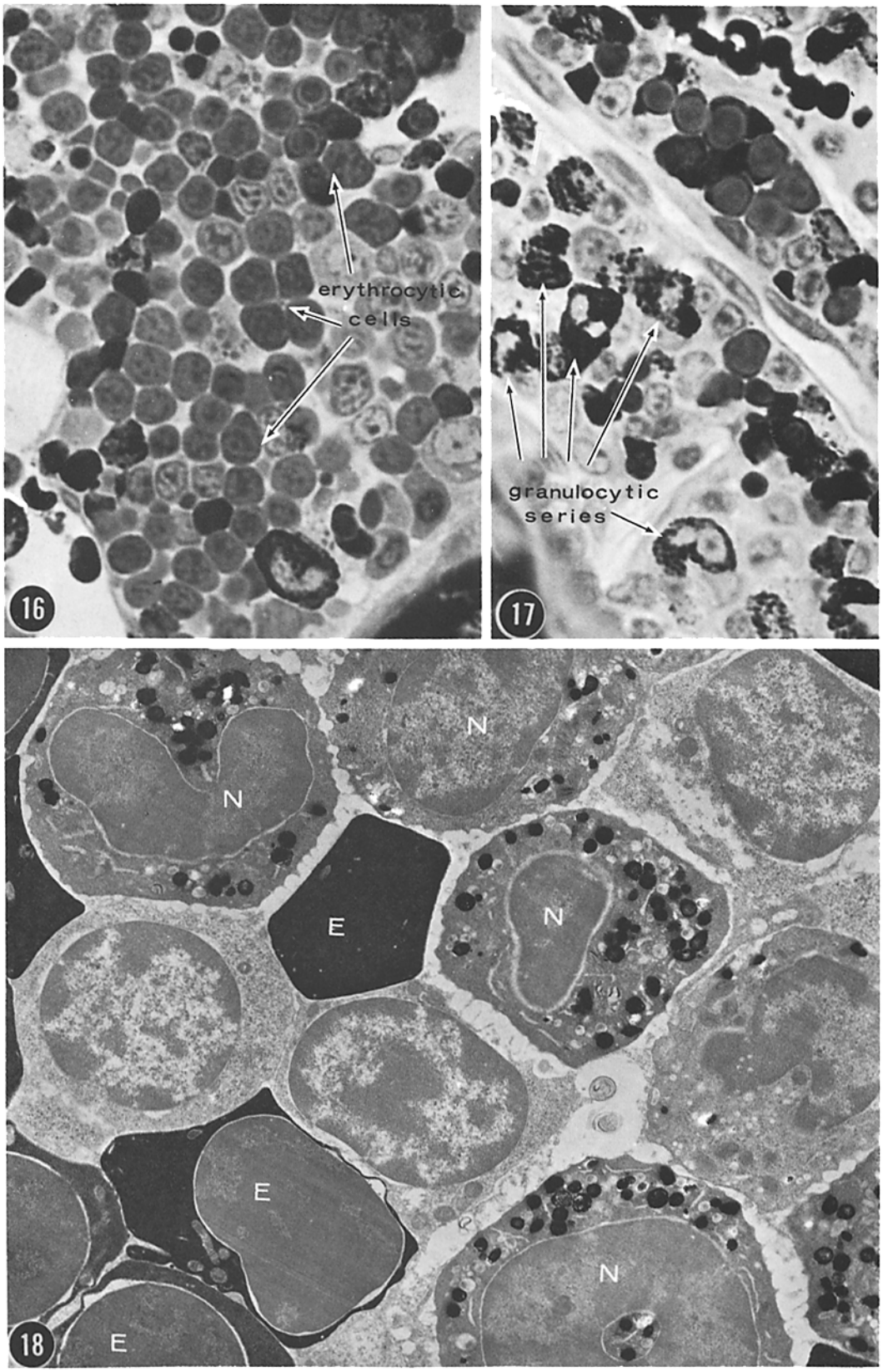

FIGURES 16 and 17 Day 21. Light micrographs of developing bone marrow stained by the diaminobenzidine-H_2O_2 procedure. The darkly stained erythrocytic cells (Fig. 16) and dense granular granulocytic cells (Fig. 17) are distinguishable. × 240.

FIGURE 18 Day 21. An electron micrograph of hemopoietic cells. Note the neutrophilic (*N*) cells with granular peroxidase-positive reaction product. Erythrocytic (*E*) series exhibit a more uniform distribution of diaminobenzidine-positive hemeprotein. × 8,000.

information locally at the site of fracture. The developmental implications and possible role of collagenous matrix in imparting positional information during embryogenesis and in repair processes, such as fracture healing in man and limb regeneration in amphibians, has been discussed previously (19, 20).

The technical assistance of Mr. K. P. Anderson, Ms. Sagami Paul, and Ms. Christine Marcus is gratefully appreciated.

This research was supported by grants from The National Foundation-March of Dimes, The American Cancer Society, Inc., Jane Coffin Childs Memorial Fund for Medical Research, and the National Institutes of Health (CA 11603 and HD 07110-02).

Received for publication 21 November 1975, and in revised form 24 February 1976.

REFERENCES

1. ANDERSON, H. C. 1969. Vesicles associated with calcification in the matrix of epiphyseal cartilage. *J. Cell Biol.* **41**:59–72.
2. BONUCCI, E. 1971. The locus of initial calcification in cartilage and bone. *Clin. Orthop. Relat. Res.* **78**:108–139.
3. BLOOM, W., and D. W. FAWCETT. 1968. *A Textbook of Histology*, 9th Edition. W. B. Saunders Co., Philadelphia, Pa.
4. CRISSMAN, R. S., and F. N. LOW. 1974. A study of fine structural changes in the cartilage-to-bone transition within the developing chick vertebra. *Am. J. Anat.* **140**:451–470.
5. GODMAN, G. C., and K. R. PORTER. 1960. Chondrogenesis studied with the electron microscope. *J. Biophys. Biochem. Cytol.* **8**:719–760.
6. GONZALES, F., and M. J. KARNOVSKY. 1961. Electron microscopy of osteoclasts in healing fractures of rat bone. *J. Biophys. Biochem. Cytol.* **9**:299–316.
7. GRAHAM, R. C., and M. J. KARNOVSKY. 1966. The early stages of the absorption of injected horseradish peroxidase in the proximal tubules of the mouse kidney; ultrastructural cytochemistry by a new technique. *J. Histochem. Cytochem.* **14**:291–302.
8. GURDON, J. B. 1974. The Control of Gene Expression in Animal Development. Harvard University Press, Cambridge, Mass.
9. HAM, A. W., and W. R. HARRIS. 1971. Repair and transplantation of bone. *In* The Biochemistry and Physiology of Bone. Vol. III. G. H. Bourne, editor Academic Press, Inc., New York. 337–399.
10. HUGGINS, C., and S. MORII. 1961. Selective adrenal necrosis and apoplexy induced by 7,12-dimethylbenz(a)anthracene. *J. Exp. Med.* **114**:741–760.
11. KARNOVSKY, M. J. 1965. A formaldehyde-glutaraldehyde fixative of high osmolarity for use in electron microscopy. *J. Cell Biol.* **27**:137a–138a (Abstr.).
12. LOWRY, O. H., N. J. ROSEBROUGH, A. L. FARR, and R. J. RANDALL. 1951. Protein measurement with the Folin phenol reagent. *J. Biol. Chem.* **193**:265–275.
13. MARTLAND, M., F. S. HANSMAN, and R. ROBISON. 1924. The phosphoric esterase of blood. *Biochem. J.* **18**:1152–1160.
14. MATUKAS, V. J., and G. A. KRIKOS. 1968. Evidence for changes in protein polysaccharide associated with the onset of calcification in cartilage. *J. Cell Biol.* **39**:43–48.
15. MOLONEY, W. C. 1958. Leukocyte alkaline phosphatase activity in the rat. *Ann. N. Y. Acad. Sci.* **75**:31–36.
16. PEASE, D. C. 1956. An electron microscopic study of red bone marrow. *Blood.* **11**:501–526.
17. PORTER, K. R., and C. V. Z. HAWN. 1949. Sequences in the formation of clots from purified bovine fibrinogen and thrombin: a study with the electron microscope. *J. Exp. Med.* **90**:225–232.
18. REDDI, A. H. 1974. Bone matrix in the solid state: geometric influence on differentiation of fibroblasts. *In* Advances in Biological and Medical Physics. J. H. Lawrence and J. W. Gofman, editors. Academic Press, Inc., New York. **15**:1–18.
19. REDDI, A. H. 1975. Collagenous bone matrix and gene expression in fibroblasts. *In* Extracellular Matrix Influences on Gene Expression. H. C. Slavkin and R. C. Greulich, editors. Academic Press, Inc., New York. 619–625.
20. REDDI, A. H. 1976. Collagen and cell differentiation. *In* Biochemistry of Collagen. G. N. Ramachandran and A. H. Reddi, editors. Plenum Publishing Corp., New York. In press.
21. REDDI, A. H., and C. B. HUGGINS. 1971. Lactic/Malic dehydrogenase quotients during transformation of fibroblasts into cartilage and bone. *Proc. Soc. Exp. Biol. Med.* **137**:127–129.
22. REDDI, A. H., and C. B. HUGGINS. 1972. Biochemical sequences in the transformation of normal fibroblasts in adolescent rat. *Proc. Natl. Acad. Sci. U. S. A.* **69**:1601–1605.
23. REDDI, A. H., and C. B. HUGGINS. 1973. Influence of geometry of transplanted tooth and bone on transformation of fibroblasts. *Proc. Soc. Exp. Biol. Med.* **143**:634–637.
24. REDDI, A. H., and C. B. HUGGINS. 1974. Cyclic electrochemical inactivation and restoration of competence of bone matrix to transform fibroblasts. *Proc. Natl. Acad. Sci. U. S. A.* **71**:1648–1652.
25. REDDI, A. H., and C. B. HUGGINS. 1975. The formation of bone marrow in fibroblast-transformation ossicles. *Proc. Natl. Acad. Sci. U. S. A.* **72**:2212–2216.
26. REYNOLDS, E. S. 1963. The use of lead citrate at high

pH as an electron-opaque stain in electron microscopy. *J. Cell Biol.* **17**:108–112.
27. ROBISON, R. 1923. The possible significance of hexosephosphoric esters in ossification. *Biochem. J.* **17**:286–293.
28. SCHENK, R. K., D. SPIRO, and J. WIENER. 1967. Cartilage resorption in the tibial epiphyseal plate of growing rats. *J. Cell Biol.* **34**:275–291.
29. SCOTT, B. L., and D. C. PEASE. 1956. Electron microscopy of the epiphyseal apparatus. *Anat. Rec.* **126**:465–495.
30. SLAVKIN, H. C. 1972. Intercellular communication during odontogenesis. *In* Developmental Aspects of Oral Biology. H. C. Slavkin and L. A. Bavetta, editors. Academic Press Inc., New York. 165–199.
31. THYBERG, J. 1974. Electron microscopic studies on the initial phases of calcification in guinea pig epiphyseal cartilage. *J. Ultrastruct. Res.* **46**:206–218.
32. URIST, M. R. 1965. Bone: formation by autoinduction. *Science (Wash. D. C.).* **150**:893–899.
33. URIST, M. R. 1970. The substratum for bone morphogenesis. *Dev. Biol. Suppl.* **4**:125–163.